COMPARISON OF PolSAR AND PolInSAR COHERENCE BASED LAND USE/LAND COVER CLASSIFICATION

Ramya M N S[1], Shashi Kumar[2]
[1] Centre for Space Science and Technology Education in Asia and the Pacific, Dehradun
[2] Photogrammetry and Remote Sensing Department, Indian Institute of Remote Sensing, Dehradun

Abstract: Classification of SAR data is a challenging as well as an essential task of continuous monitoring of the earth's surface due to its all-weather capability**.** This paper investigates PolSAR and PolInSAR coherence concept for the extraction of the earth features. The methodology integrated with Polarimetric decomposition models, PolInSAR Coherence, Mahalanobis and Knowledge based classification for land use and land cover (LULC) classification using fully polarimetric RADARSAT- 2 data. Polarimetric decompositions helped to investigate and understand the scattering mechanism patterns to extract the information of the earth's features. Freeman, Yamaguchi and H/A/Alpha decomposition models were used to extract different scattering mechanisms. The results shown overestimation of the volume scattering in highly dense and oriented building, this leads to misinterpretation of these buildings as forest in PolSAR classification. This issue is addressed by incorporating PolInSAR coherence, which is sensitive to both volumetric structure and temporal change of the scatterer. Forest regions were strongly affected by the temporal and volume decorrelation with time, which show low coherence values compared to the permanent scatterers like built-up areas. The backscatter response and the coherent patterns of vegetation compared to urban area are different, this helped to extract built-up regions more accurate. Therefore, PolInSAR coherence is utilized for extraction of the features by combining polarimetric and coherence information. The PolInSAR coherence extracted from the repeat-pass RADARSAT-2 images of 24 days temporal baseline for distinguishing vegetation and built-up areas. The Mahalanobis classification algorithm was used for extracting different features. To further improve the results, Knowledge based classification was executed by forming rules based on the statistical analysis of the features. The overall accuracy and kappa statistics of the PolSAR and PolInSAR Coherence classification are 79.17% and 0.75, 86.67% and 0.84 respectively. This states that PolInSAR coherence classification helped to characterize discrete and volume scatterers more accurately than the PolSAR classification.

KEYWORDS: PolSAR, PolInSAR Coherence, Polarimetric decomposition model, Mahalanobis classification and Knowledge based classification.

1. INTRODUCTION:

Land is the most precious resource available on the earth's surface which covers an area of 149 million km² whereas India landmass covers 3.28 million km^2 (universetoday website). LULC are the two prominent land surface features on the earth's surface. Land cover is the physical cover of the earth's surface like water bodies, forest, rocks and bare soil. Land use is defined as a series of operations carried out by the humans, for extracting some product or benefit using the land resource like agriculture, industries. The study of LULC has become an interesting and important research topic to overcome problems like the unsustainable use of the natural resources, loss of wildlife habitat, prime agricultural lands and deteriorating environmental quality (Anderson *et al*, 1976). LULC changes caused by human activities are due to the rapid growth in the population, increasing demand for the agriculture, urbanization and economic development and natural processes like natural disasters. LULC map is needed for the analysis of environmental processes, to improve living conditions, sustainable development of the resources and analysis of LULC change. Traditional methods for gathering demographic data, censuses, and analysis of LULC samples are not adequate for mapping as it has problems like time consuming, complexity in data handling from different sources (Maktav *et al*, 2005). Therefore, advanced technologies like Remote Sensing and Geographical Information Systems became an important tool to monitor the dynamics of natural resources in the fields of agriculture, environments and geology.

Remote sensing technology plays a major role in LULC mapping as it consumes less time, low cost and classifies with better accuracy (Kachhwala, 1985). Remote Sensing satellites provide wide data from different sources regarding the same area at different spatial, spectral and temporal resolutions. However, optical remote sensing is affected by the cloud cover due to its low wavelength and depends on the solar illumination which makes it difficult for continuous monitoring of the earth's surface. As India is a tropical country is affected by the cloud cover, due to which low availability of usable optical images. These constraints can be overcome by the use of microwave remote sensing as it penetrates through clouds, haze, dust, independent of solar illumination and all-weather capable. Advances in microwave remote sensing improved the measuring capability by operating the Radar in multiple frequencies and polarizations. Synthetic Aperture Radar (SAR) data has become an important source for LULC mapping and monitoring. Backscattering values of the features that variates with the change in polarization and incidence angle. Therefore, SAR image classification became an important research topic in the scientific field, facing many challenges.

Several polarimetric parameters were developed from the SAR data like backscattering coefficients and scattering decompositions. Understanding these polarimetric parameters and its significance for monitoring various LULC features is important. SAR backscatter from the earth's surface depends on the sensor parameters like wavelength, polarization, incidence angle as well as target parameters like surface roughness, dielectric constant and feature orientation. Classification based on the backscattering values in a single polarization of SAR is affected due to the speckle and limited information from the resolution cell consisting different scatterers. (Wang *et al*, 2016) Compared qualitatively and quantitatively the performance of full, dual and single polarization of SAR data in classification of LULC. This study concluded that single polarization SAR data is poor in classification because of the limited backscatter and texture information. Fully polarimetric data extracts information in different polarizations like HH, HV, VH and VV polarizations, which helps in the better characterization of the target. To enhance the capability of SAR data classification backscattering values in different polarizations are integrated using polarimetric SAR (PolSAR) data. Polarimetric decomposition models separates the total backscatter power from a single SAR pixel into different physical scattering mechanisms such as surface, double bounce and volume scattering. Surface scattering is observed when the wave reflected from the surface, double bounce scattering is due to the wave interacting orthogonal surfaces with different dielectric constant and volume scattering is observed from randomly oriented dipoles like tree canopy. Incoherent decomposition models like H/A/Alpha, Freeman-Durden and Yamaguchi decomposition models are considered in this study, they are derived from the second order derivatives of the scattering matrix known as coherency or covariance matrix (Cloude, 1996).

Polarimetric Interferometric Synthetic Aperture Radar (PolInSAR) is an advanced area of research which had significant consideration from the mid of the year 1990. This research area has combined the utility of two SAR technologies: Polarimetric SAR (PolSAR) and Interferometric SAR (InSAR) became well developed techniques (Cloude and Pottier, 1996, Cloude and Papathanassiou, 1998 and Yamada *et al*, 2002, 2009). Polarimetric InSAR (PolInSAR) permits a distinction between different distributed targets at different elevations. InSAR technology combines the two complex SAR signal of the same area acquired from two slightly different look angles or at different times. The combination of two coherent SAR images are used to extract the information about the phase difference and the coherence magnitude that provides information about the interferometric phase difference quality. Coherence is the measure of local phase correlation between two complex SAR images (Catherine and André, 2007). The interferometric coherence depends on the sensor parameters (wavelength, system noise and resolution), imaging geometry (interferometric baseline, local incidence angle) and the target parameters (Abdelfattah and Nicolas, 2006). PolInSAR coherence contains the full set of polarimetric and interferometric information, which became an important parameter for number of applications. It is strongly polarimetric dependent and many studies explored its application for forest terrain analysis, man-made feature identification and for single and multi-baseline PolInSAR configurations. PolInSAR complex coherence helps to reconstruct the vertical profile function in penetrable volume scattering (Cloude, 2006, 2007). It is a parameter that is sensitive to both the volumetric structure of the scatterers in the resolution cell and to temporal change processes (Neumann, 2008). Forest terrains suffer strongly by the temporal and volume decorrelation due to which they show low coherence value compared to the permanent scatterers like built-up area. As PolInSAR coherence exhibit close relationship with the forest structures, so they are explored for the parameter retrieval. Based on these facts, PolInSAR coherence concept is considered for the extraction of man-made and natural features.

A variety of classification techniques are developed for LULC classification and monitoring using remotely sensed data. Classification techniques classify groups of pixels in the image to represent LULC features like forest, urban, agricultural, water, bare soil and river bed. They are categorized into two approaches, namely unsupervised and supervised algorithms. Unsupervised classification groups the pixels into classes based on the reflectance properties of the pixel. It is accomplished by identifying clusters of the measured feature vectors, and by designating each distinct cluster as a new class. This automatic operation helps for real-time processing's but show lower performance than the supervised classification. Supervised algorithms train the classifier using the training data provided by the analyst, it estimates the statistics or parameters for each feature class. The accuracy and number of classes to be classified depends on the samples selected by the analyst. This classification includes different algorithms like minimum distance (Wacker *et al*, 1972) and Mahalanobis distance classifier (Paul Mather *et al*, 2009). Mahalanobis classifier is focused in this study, to further improve the classification accuracy segmentation and knowledge based approach are applied in the methodology.

2. STUDY AREA AND DATASET:

The site selected is a part of Uttarakhand which lies in the northern part of the India. This area was chosen due to its diverse LULC and varying topography. This area includes forests, settlements along with agriculture as well as water bodies like Ganga river. Man-made features such as large building blocks are present in Rishikesh, Doiwala and Balawala. Buildings in the Doiwala and in rural Rishikesh represented as dominant double bounce scattering, but few shown dominance in volume scattering instead. These urban areas are covered with highly dense buildings along with

small plants between the built up region. Forest and agriculture contribute to the volume scattering due to its structure of the canopy leading to the multiple reflections. The high mountains and rugged terrain in the eastern zone of the image were used to observe the variation of scattering powers with topography. As this area includes different type of scatterers exhibiting different scattering dominance is chosen for the study. Radrasat-2 data operated in C-band of wavelength 5.55cm is considered for this study. Interferometric pair acquired on 3rd and 28th March 2013 in Fine Quad-polarization with similar geometrical configuration over a temporal baseline of 24 days. The study area and dataset were shown in the Figure 1.

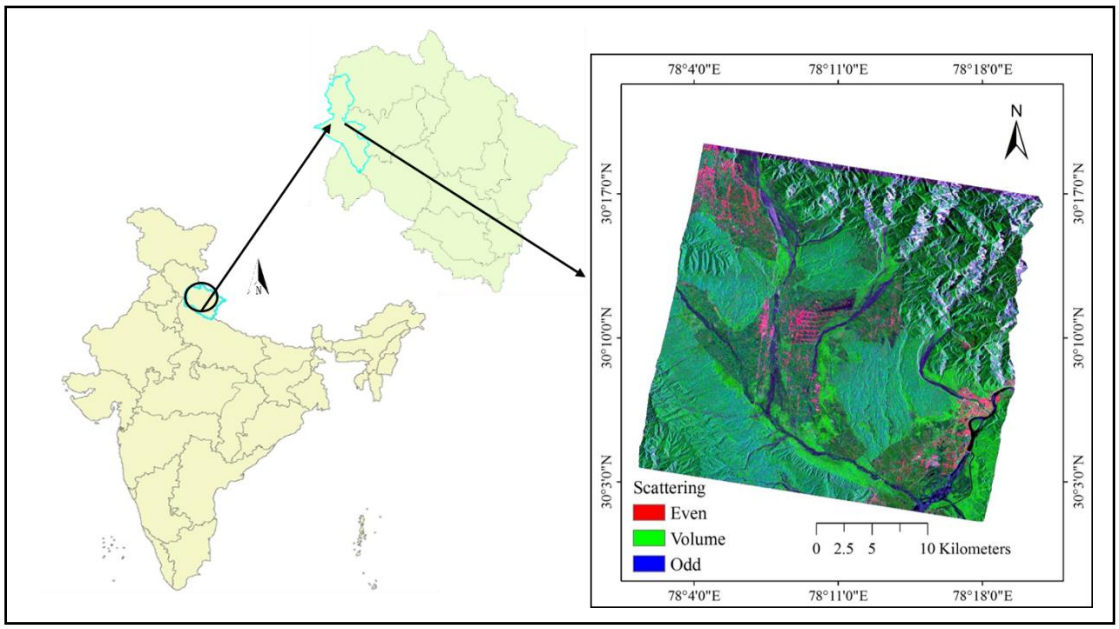

Figure 1: RADARSAT-2 data of the study area.

3. METHODOLOGY:

3.1 Pre-Processing Steps:

Radrasat-2 data has to be preprocessed before applying the classification techniques. The pre-processing includes different steps like radiometric calibration, multi-looking, generation of the scattering and coherency matrix. Absolute radiometric calibration for RADARSAT-2 is calculated based on the sigma nought, gamma nought and beta nought look up tables provided in the dataset. As the SAR acquisition are side-looking sensors, measures the distance between the objects and also the distance from the sensor in the slant range direction. The objects in near range appear to be compressed as compared to the object in the far range. This effect can be removed by the process of converting a slant range to ground range resolution known as Multilooking. The number of looks is a function of pixel spacing in range direction, azimuth direction and incidence angle. The pixel spacing in range direction is 4.733 m, azimuth direction is 4.84 m and incidence angle is 40^0. The number of looks in Azimuth direction is 2 and Range direction is 1. Multilooking process converts approximately into square pixel of 8.52 meters.

In the SAR resolution cell there are different types of scatterers. The return signal from these scatterers is coherently summed to obtain the phase and brightness of the resolution cell. Due to the very strong reflector at specific alignment or coherent sum of signal reflected from different scatterers, shows very high brightness values than the actual brightness caused by the object in a resolution cell. This high brightness values of the resolution cell appears as speckle on the SAR images. This is an often problem with the Radar image, which is to be reduced for further quantitative analysis of the data. Speckle filtering is a method to reduce speckle from the image. There are different filters like Box car filter, Gamma map filter, Refined Lee filter etc. of different size (Lee *et al*, 1994). The selection of the window size is important and data oriented, selection is based on the edge preservation, speckle reduction, preservation of texture information and should not blur the image (Nyoungui *et al*, 2002). In this study, Gamma-Map with window sizes of 3x3, 5x5 and 7x7 are examined. A comparative analysis by visual interpretation of the filtered images is carried out and Gamma-Map with window sizes of 5x5 is selected. Coherency matrix [T] is generated from the scattering matrix based on the pauli vector. Based on the coherency matrix, polarimetric information is extracted from the H/A/Alpha, Freeman and Yamaguchi decomposition models for performing classification.

3.2 Decomposition Models:

3.2.1 Yamaguchi Decomposition Model: Freeman and Durden developed a three-component physical based scattering mechanism decomposition model in 1998 to represent different features on the earth's surface (Freeman *et al*,1998). The model included scattering from a cloud of randomly oriented dipoles known as volume scattering, scattering from a pair of orthogonal surfaces with different dielectric constants called double bounce scattering and Bragg scatter from surface represented as odd bounce scattering. Freeman assumes the reflection symmetry condition, which states that $S_{HV}\,S^{*}_{VH} = S_{VV}\,S^{*}_{HV} = 0$. This condition is not valid for the oriented buildings. The drawbacks in this model are assumed of reflection symmetry and the selection of inappropriate volumetric scattering models. Therefore, to overcome this problem Yamaguchi developed a four component decomposition model. To remove the assumption of reflection symmetry, introduced a fourth scattering component called as helix scattering and similar scatterings included as those in the Freeman model. This helix scattering term is observed in complex urban areas and it is negligible for naturally distributed scatterers such as agricultural fields and forest. Yamaguchi decomposition model separates the total backscatter power as a sum of surface, double bounce, volume and helix scattering (Yamaguchi *et al*, 2005). The expression for Yamaguchi decomposition is shown in the equation (1).

$$[T] = P_s[T]_{surface} + P_d[T]_{double} + P_v[T]_{volume} + P_c[T]_{helix} \quad (1)$$

Where, $[T]$ is the coherency matrix, Ps, Pd, Pv, Pc corresponds to the power of scattering mechanism and they are the expansion coefficients of surface, double bounce, volume and helix scattering.

3.2.2 H/A/Alpha Decomposition Model: The H/A/Alpha decomposition model is based on the eigenvalue decomposition of the coherency matrix, entropy, alpha and anisotropy parameters are computed in this model. Entropy is a measure that indicates the randomness in the target vector. For pure targets entropy equals to zero, whereas for distributed targets represent values close to 1. Alpha indicates average or dominant scattering mechanism in terms of volume, double bounce or surface scattering based on the angle of Eigen vector. Low values of alpha are interpreted as surface scattering, 45^0 indicates depolarizing feature like forest and near to 90^0 represents double bounce scattering. Anisotropy is the relative importance between the second and third eigenvector. The low value of the anisotropy indicates one dominant scattering mechanism, whereas a high value indicates two dominant scattering mechanisms with equal probability or with less significant third scattering mechanism.

3.3 PolInSAR Coherence:

The interferometric coherence (γ) is defined as the absolute value of the normalized complex cross correlation of interferometric pair. Interferometric coherence is a function of coherency matrix and polarization basis (Cloude and Papathanassiou, 1998).

$$\gamma = \frac{\langle \omega_1^{*\mathrm{T}}[\Omega_{12}]\omega_2 \rangle}{\sqrt{\langle \omega_1^{*\mathrm{T}}[\mathrm{T}_{11}]\omega_1 \rangle \langle \omega_2^{*\mathrm{T}}[\mathrm{T}_{22}]\omega_2 \rangle}} \quad (2)$$

Where $\omega_1$and ω_2 represents two scattering mechanisms, * indicates complex conjugation and the angular brackets represent spatial averaging over a selected window size. The modulus of coherence indicates the degree of correlation between these two images and the argument of γ is the interferometric phase difference. It is affected by different decorrelation parameters such as spatial baseline, processing errors like co-registration, signal noise, temporal correlation between the acquisitions and volume decorrelation due to the vertical distribution of the scatterers like forest and plantation.

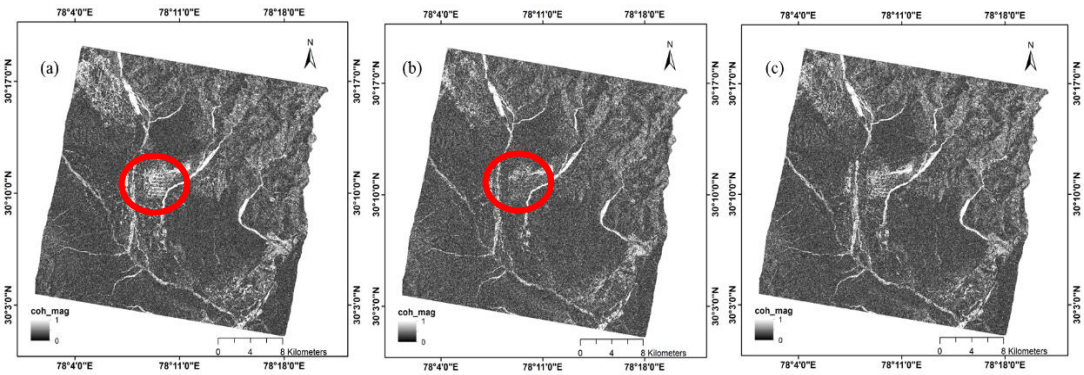

Figure 2: (a) HH Coherence (b) HV Coherence and (c) VV Coherence.

In this technique, coherence images were obtained of different linear combinations of H, V-polarization basis i.e. HH, HV and VV elements of the scattering matrix were shown in the Figure 2. High coherence values were observed in the dry riverbed and settlements as they are visible in a brighter tone compared to the other features. However, low coherence is observed in Forest and agriculture due to the effect of temporal and volume decorrelation (Cloude and Papathanassiou, 1998). Settlements shown high coherence in HH and VV polarizations which indicates that the features is stable and there is negligible volume and temporal decorrelation. The coherence for settlements is lower in HV polarizations compared to HH and VV polarizations which is highlighted by the red circles in Figure 2 (a) and (b). As they are solid structures contribute to high backscattering in HH and VV polarization and negligible cross-polarization. This leads to high values in HH and VV coherence. For forest regions, the coherence is very low in all the three polarizations represented as dark tone. Buildings which are closely spaced or highly oriented undergoes multiple reflections and contribute to the cross polarization. This type of settlements shows high coherence in all three polarizations observed near the Ganga river of Adarsh nagar whereas built up area near the Pashulok colony showing high coherence only in HH and VV polarization. The agriculture and bare land have shown low coherence values and represented as darker tone. The Barkot, Lachhiwala, Motichur and Thano forest ranges are exhibiting very low coherence in all three polarizations resembling darker shades.

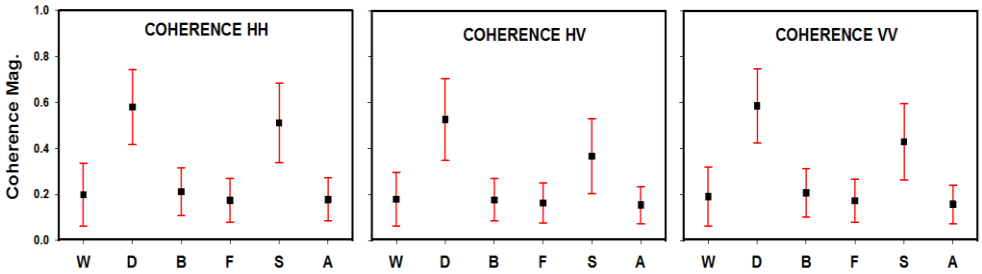

Figure 3: Coherence magnitude ranges in different linear polarization for different features.

Figure 3 represents the range of the coherence value of different features in H, V polarization. The black mark in the graph represents the mean coherence value of the feature and red bars represent the standard deviation of the range. The coherence magnitude value ranges from 0 to 1, high coherence is shown by the stable features. W represents the water, D represents the dry riverbed, B represents for the bare land, F represents forest, S represents settlements and A represents Agricultural fields. Water features shown low coherence in all three polarizations ranging from 0.05 to 0.35. Riverbed shown higher value than the other features ranging from 0.3 to 0.8, bright in all coherence maps. The bare land value ranges from 0.1 to 0.3 in all coherence maps, which are affected by the temporal decorrelation. Settlements shown higher values 0.35 to 0.7 in HH and VV coherence whereas in HV coherence ranges from 0.26 to 0.57. Vegetation i.e. Forest and agricultural fields shown low coherence range from 0.1 to 0.3 compared to the other features as it is highly affected by both temporal and volume decorrelation. The dependency of the coherence on the polarization leads to a typical variation of the coherence with the polarization and feature type. Therefore, Cloude solved the problem of polarization dependent in 1998 by the introduction of the optimization techniques. These techniques helped to maximize the coherence values and reduce the Interferometric noise. To solve the coherence optimization problem, the modulus of a complex Lagrangian function L should be maximized:

$$L = \underline{W_1^{*T}}\Omega_{12}\underline{W_2} + \lambda_1\left(\underline{W_1^{*T}}\mathrm{T}_{11}\underline{W_1} - 1\right) + \lambda_2\left(\underline{W_2^{*T}}\mathrm{T}_{22}\underline{W_2} - 1\right) \quad (3)$$

The L function is solved by the eigen values and generate three coherence optimal bands i.e.$\gamma_{opt1,}\gamma_{opt2}$ andγ_{opt3}. Their coherence magnitudes can be represented as:

$$1 \geq \gamma_{opt1} \geq \gamma_{opt2} \geq \gamma_{opt3} \geq 0 \quad (4)$$

Figure 4 represents RGB view of the coherence optimal bands and its histogram. Forest regions resembled in the darker tone compared to all other features whereas dry riverbed represented by the brighter tone. Settlements are represented by two different signatures like white and reddish shade as it is shown low value in Opt-3 visible. The mean values of the coherence Opt-1 are the highest, then followed by the coherence Opt-2 and then by coherence Opt-3.

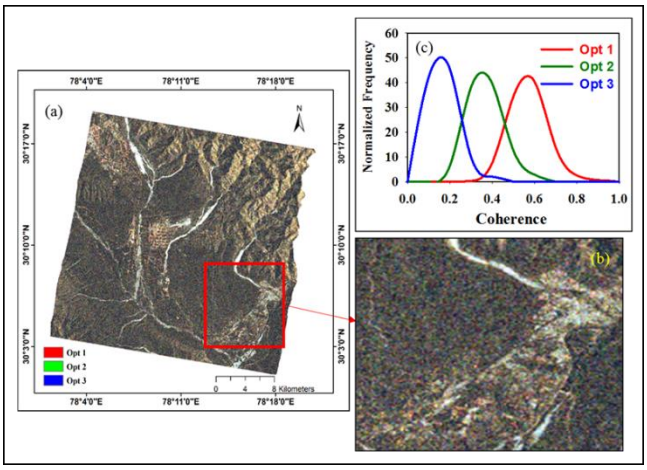

Figure 4: (a) A color composite coherence image for optimal polarization basis, (b) zoomed part of the color composite image and (c) histogram of three coherence optimal bands.

3.4 Classification:

The Supervised classification technique is chosen as the analyst has the prior knowledge of the study area and defined the required classes to be classified. Once the training sites were determined, a supervised classification was performed using a Mahalanobis distance algorithm. Land classification scheme selected to classify this image is of level-1 which includes features like water, forest, agriculture, settlement, bare land and riverbed. Water category comprises areas covered with surface water or impounded in the form of ponds, reservoirs or flowing as rivers, canals etc. Forest or shrub land are the areas covered with mature trees, shrubby plants and other plants growing close together. There are different type of forest like evergreen forest, deciduous forest etc. Agricultural area is a land use feature which provides land for food production over a period of time. These are the areas with standing crop as on the date of the satellite overpass. Settlements are defined as an area of human habitat developed for residential, commercial, industrial, transportation and other facilities. The built-up land of study area comprises Rishikesh, jolly grant airport, doiwala etc. Bare lands included lands which are not in use as they are degraded due to agricultural activities, Mountainous or hilly areas and includes areas with no vegetation cover. Dry riverbed is a channel bed through which river floats during heavy rains. These classes are considered in defining the training classes for the supervised classification.

Mahalanobis distance classification is a supervised classification, which is introduced by Mahalanobis in 1936. It is a direction sensitive distance classifier based on the statistics of the features. This is a mean clustering algorithm, decision rule adopted by the minimum distance classifier to determine pixels label in the minimum distance between the pixel and class centres based on the Mahalanobis distance (Paul Mather *et al*, 2009).

$$D_M = \left(X_i - \mu_j\right)^T \cdot C_j^{-1} \cdot \left(X_i - \mu_j\right) \quad (5)$$

Where, D_M is the Mahalanobis distance, T denotes transpose of matrix, C_j^{-1} denotes inverse of variance-covariance matrix for cluster j, X_i is the observed vector of the ith pixel and μ_j is the mean of the jth cluster. The mean spectral vector and variance-covariance parameters are determined from the training dataset of the classes. A pixel is labelled by computing the distance between the pixel and each class centroid. The label of closest centroid is then assigned to the pixel. Based on this criteria each pixel of the image is classified into the class. In the special cases, where the features are uncorrelated and the variances in all directions are the same, then the Mahalanobis distance algorithm becomes equivalent to the Euclidean distance. The mahalanobis overcomes the limitations of the Euclidean distance algorithm as it automatically accounts for the scaling of the coordinate axes, corrects for correlation between different features and provide curved as well as linear decision boundaries between the features.

As SAR images are affected by the speckles, speckle filtering helps to reduce but doesn't remove completely. Due to this the classification results are affected, to overcome this problem segmentation method is applied in this methodology as it is an object oriented classification. Segmentation partitions the classified image into regions of connected pixels and the pixels which are in the same class. Subsequently, adjacent pairs of image objects are merged to form bigger segments based on the homogeneity criteria between the pixels. The homogeneity criterion is a combination of spectral values and shape properties. After segmenting the classes, different morphological operators like clump and sieve are applied based on the feature. Morphological image processing is a collection of non-linear

operations related to the shape or morphology of features in an image. Clump operator is used to cluster the adjacent similar classified areas together into a single class. As the classified images often suffer from speckles, gaps are formed in between the features. This can be overcome by the use of low pass filtering or clump operator. But the Low pass filtering smoothens the image and adjacent classes are misclassified (Lillesand, 1979). Therefore, clumping operator is chosen to solve this problem. The classes are clumped together by first performing a dilate operation followed by the erode operation on the classified image using kernel of the size specified by the analyst. Sieve operator used after the application of the clump, considered to remove the problem of the isolated pixels occurring in classification images (Quinlan *et al,* 2006). If the number of pixels in a class that are grouped is less than the value specified by the analyst, those pixels will be removed from the class. After the segmentation, a set of knowledge-based classification rules is executed to describe the each class.

Knowledge based approach is a part of artificial intelligence and is considered one of the high level methods. The most commonly used techniques for knowledge representation in image classification are rule-based approach and neural network classification (Amarsaikhan *et al,* 2012). In the present study, for discrimination of the LULC features a rule-based approach has been applied. It uses a hierarchy of rules, or a decision tree describing the conditions under which each feature is separated from the other features. The Decision tree is composed of root nodes, a set of interior nodes and terminal nodes. The classification process has been implemented by a set of rules that determine to be followed, starting from the root node and ends at terminal node. At each non-terminal node, a decision has to be made about the path to the next node. The nature of decisions being set and the sequence of attributes occurring within a tree will affect the classification. In this approach, a statistical analysis of all the features are done and estimates of the decision boundaries are derived to design classification tree. The constructed rule-based approach consists a set of rules, constraints on spectral parameters and spatial thresholds. The spectral thresholds were determined based on the analysis about the spectral characteristics of the selected classes. Terminal nodes of the decision tree represent classified features of the image.

4. RESULTS AND DISCUSSION:

In PolSAR based classification, backscattering in all polarizations and scattering mechanisms extracted from decomposition models were considered. Mahalanobis distance classification is applied to the SAR dataset to classify six classes based on the training data of classes as specified in the section 3. Water has a smooth surface due to which it gives specular reflection and show low backscattering compared to the other features in all polarizations. These areas were identified and mapped as water bodies represented in the blue color. But SAR images in hilly terrain are affected by the shadow, layover and foreshortening, due to which they show low backscattering similar to the water bodies. Therefore, few pixels in the hilly terrain are misclassified as water bodies. Forest is a cloud like object consisting randomly oriented dipoles due to which they are dominant in volume scattering. As RADARSAT-2 operates in C-band which is of low wavelength, cannot penetrate through the canopy. It interacts with the top layer of the canopy due to this reason it shows high values even in odd bounce scattering. Few pixels of the forest are mixed with the pixels of riverbed. Settlements are dihedral structures show high values in the double bounce scattering. They are represented in the red color in the classified image, but few oriented buildings are misclassified into the forest as they show dominant volume scattering. River bed shows high values in the odd bounce scattering and represented by the cyan color in the classified image. Agriculture are moderate in volume scattering and represented by the yellow color in the classified image. Bare land gives surface scattering and they are represented by the brown color in the classified image.

Few classes were misclassified, therefore knowledge based classification and different morphological operators like clump and sieve were applied to improve the classification. Forest cover large area compared to the other features, few pixels in the forest are misclassified as river bed and agriculture. To overcome this segmentation is applied, to fill the gaps in the feature clump operator of size 5x5 has been used for forest. Water accuracy is affected due to the hilly terrain in the study area. This is overcome by considering the elevation parameter of the study area. The knowledge based rules to classify features more accurately were executed based on the statistical analysis like "elevation LT 600" for water, "elevation GT 650". Mixed pixels in the forest are minimized comparatively, rules like "Radar Vegetation Index greater than 0.5", "Alpha less than 36", "Beta less than 48" and "Volume scattering greater than 0.88" are executed. In hilly terrain, forest is misclassified as agriculture to separate them "elevation greater than 600" is executed. Rules like "Double bounce scattering greater than 0.1", "Alpha greater than 44" and "Anisotropy greater than 0.33" for settlements, "Elevation less than 600", "Volume scattering less than 0.085" and "HV Backscattering greater than -20" for agriculture and "Alpha LT 36" for Bare land. Few oriented buildings are still

misclassified into the forest, no rule is able to separate them. The classified map of the PolSAR is represented in the Figure 5 (a).

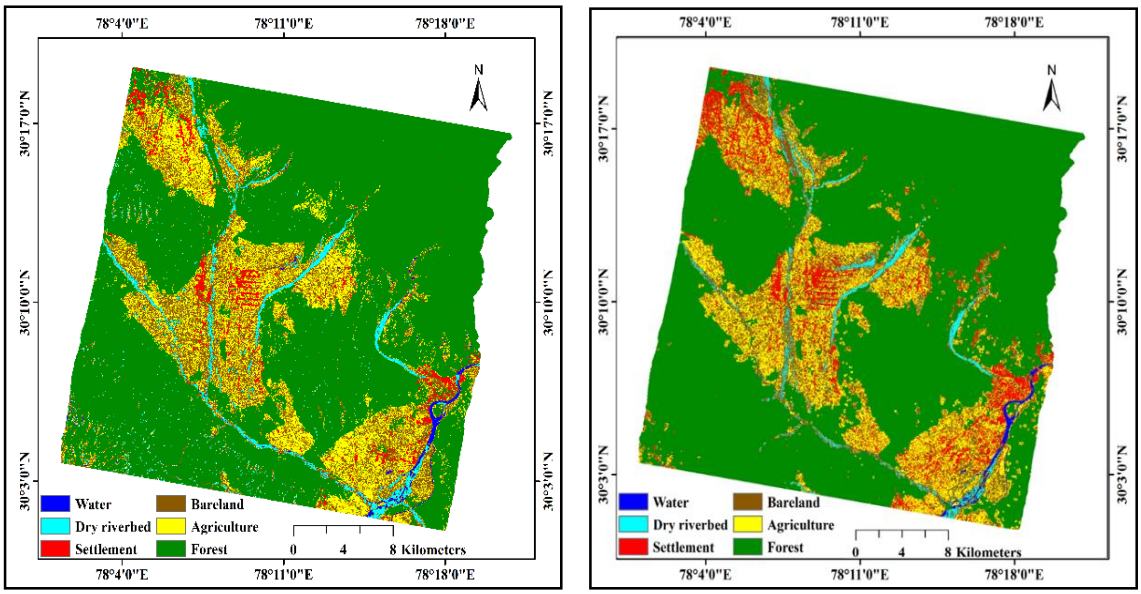

Figure 5: (a) PolSAR Classified Map and (b) PolInSAR Classified Map.

In PolInSAR classification, Interferometric Coherence in different polarizations, Backscattering coefficients and polarimetric decomposition model of master and slave were considered. The rules considered in PolInSAR classification after Mahalanobis algorithm were "elevation less than 600" for water, "elevation greater than 620", "Alpha less than 39.2" and "Volume scattering greater than 0.088" for forest, "Anisotropy based on coherence greater than 0.132", "Double bounce scattering greater than 0.03", "Double bounce scattering greater than Odd bounce scattering" and "Opt-1 greater than 0.6" for settlements, "Opt-1 less than 0.6", "Elevation less than 600" and "Volume scattering greater than 0.05" for agriculture and "Odd and Double bounce less than Volume scattering", " HH coherence less than 0.5" and "Alpha less than 36" for Bare land. The classified map of the PolInSAR is represented in the Figure 5 (b). As seen from the classified map, the rule-based approach helped to separate objects accurately.

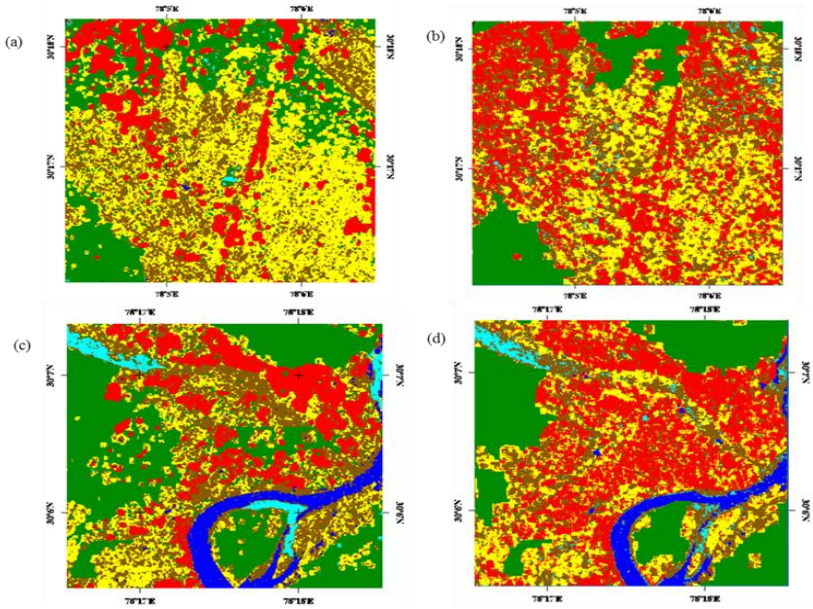

Figure 6: (a), (c) PolSAR and (b), (d) PolInSAR classified map of Pratimayan Chowk and Rishikesh.

From PolSAR and PolInSAR classified map, it can be observed that forest is misclassified into vegetation, urban and riverbed in PolSAR data. This is due to the fact that RADARSAT-2, C-band data the wave cannot penetrate into the canopy of the forest. But the data acquired in the leaf fall period, it interacts with the branches, ground and trunk which leads to dominance in odd and double bounce scattering. Due to the hilly terrain and side looking SAR sensors there was a shadow affect in the forest area. This affect was minimized with the help of digital elevation model. As

the river bed and urban show high coherence than the other features, PolInSAR classification separated them from the other features more accurately compared to the PolSAR classification. This misclassification is decreased comparatively by the consideration of the PolInSAR coherence for classification in PolInSAR coherence based classification. For better illustration two particular areas of the study area were zoomed and shown in the Figure 6, built up regions near Pratimayan chowk and Subash nagar in Rishikesh. It can be observed that in PolSAR classified map, settlements are misclassified as agriculture and forest in Figure 6(a) and (c) whereas in (b) and (d) settlements are more accurately extracted due to the inclusion of the coherence. This states that coherence parameter helps to characterize the discrete and volume scatterers. Therefore, the problem with the existing decomposition models is modified by the insertion of the coherence parameter.

Table 5. 1: Accuracy Assessment of PolSAR and PolInSAR classified map

Classes	***PolSAR classification***			***PolInSAR classification***		
	Producer's accuracy	**User's accuracy**	**Kappa statistics**	**Producer's accuracy**	**User's accuracy**	**Kappa statistics**
Water	97.83	75	0.71	94.74	90.2	0.88
Agriculture	60.27	73.33	0.67	89.47	85.52	0.82
Dry riverbed	76.36	89.67	0.89	77.27	85.46	0.82
Forest	72.33	79.67	0.73	81.82	90.32	0.88
Settlement	85.71	70	0.65	88.89	80.23	0.76
Bare land	81.48	73.33	0.68	90.00	88.91	0.88
	Overall accuracy=**79.17**		**0.75**	Overall accuracy=**86.67**		**0.84**

The error matrix is generated to measure the accuracy of the LULC mapping. It is a square array representing different features set out in rows and columns that expresses the number of samples assigned to a particular category in one classification relative to the reference data" (Qin, 2013). From the error matrix, producer's accuracy, user's accuracy, overall accuracy and Kappa statistics were calculated. Producer's accuracy measure number of pixels correctly classified in a particular category, whereas user's accuracy compute the number of correctly classified pixels to the total number of pixels assigned to a particular category. Overall accuracy is the sum of the number of correctly classified samples divided by the total number of samples in the entire error matrix. Kappa statistics analysis is a discrete multivariate technique for accuracy assessment, which measures agreement of the accuracy. Stratified random sampling method is considered for the collection of samples. Overall, 360 Testing Samples have been selected for the accuracy assessment of the classified map, 60 samples for each class. The accuracies for different features of the classified map were represented in the Table 1. The overall accuracy and kappa statistics of the PolSAR and PolInSAR classified map are 79.17% and 0.75, 86.67% and 0.84 respectively. The accuracy of the features increased in PolInSAR classification compared to the PolSAR classification. This proves that the PolInSAR coherence helped to increase the accuracy of classification in LULC mapping.

5. CONCLUSION:

This paper focuses on the capability of fully polarimetric data and PolInSAR Coherence for LULC classification by Mahalanobis and Knowledge based algorithms. The backscattering coefficient, Yamaguchi and H/A/Alpha decomposition parameters of PolSAR and PolInSAR coherence provided multidimensional information about the LULC features. Gamma map filter of window size 5x5 reduced the effect of speckles in the dataset up to some extent. Mahalanobis algorithm classified the dataset into six classes, but few pixels are misclassified to overcome this problem segmentation and Knowledge based classification were applied. Segmentation helped to eliminate the inherent speckle noise effect in the classification and classified feature as object based. The segmentation and morphological operators are suitable for the extraction of LULC features from polarimetric SAR images. Polarimetric parameters were used to interpret the scattering mechanisms of each class and to define the rules for different features. In PolSAR Classification, settlements are misclassified into the forest as they are closely spaced. Therefore, PolInSAR Coherence was considered as settlement has high values while forest show low values due to temporal and volume decorrelation. Knowledge based classifier uses its own classification rules applied sequentially to separate each class at different hierarchical levels. The overall accuracy and kappa statistics of the PolSAR and PolInSAR classified map are 79.17% and 0.75, 86.67% and 0.84 respectively. This indicates that PolInSAR classification helped to improve the accuracy of LULC classification mainly settlements.

REFERENCES

Abdelfattah, R., and Nicolas, J. M., 2006. Interferometric SAR coherence magnitude estimation using second kind statistics. IEEE Transactions on Geoscience and Remote Sensing. 44 (7), pp. 1942–1953.

Amarsaikhan, D., Ganzorig, M., Saandar, M., Blotevogel, H. H., Egshiglen, E., Gantuya, R., Nergui, B., and Enkhjargal, D., 2012. Comparison of multisource image fusion methods and land cover classification. International Journal of Remote Sensing, 33 (8), pp. 2532-2550.

Anderson, J. R., Hardy, E. E., Roach, J. T and Witmer, R. E., 1976. A land use and land cover classification for use with remote sensor data. U.S. Geological Survey Professional Paper 964, Washington.

Catherine, B., and André, O., 2007. The use of sar interferometric coherence images to study sandy desertification in southeast niger: Preliminary results. European Space Agency. Special Publication ESA SP. 636, pp. 1–5.

Cloude, S. R., and Pottier, E., 1996. A review of target decomposition theorems in radar polarimetry. IEEE Transactions on Geoscience and Remote Sensing, 34 (2), pp. 498-518.

Cloude, S. R., and Papathanassiou, K. P., 1998. Polarimetric SAR interferometry. IEEE Transactions on Geoscience and Remote Sensing. 36 (5), pp. 1551–1565.

Cloude, S. R., 2006. Polarization coherence tomography. Radio Sciences, 41 (RS4017), pp. 1–27.

Cloude, S. R., 2007. Dual-baseline coherence tomography., IEEE Transactions on Geoscience and Remote Sensing Letters. 4 (1), pp. 127–131.

Freeman, A., and Durden, S. L., 1998. A three-component scattering model for polarimetric SAR data. IEEE Transactions on Geoscience and Remote Sensing, 36 (3), pp. 963–973.

http://www.universetoday.com/25756/surface-area-of-the-earth, Retrieved on 15th November, 2016.

Kachhwala, T. S., 1985. Temporal monitoring of forest land for change detection and forest cover mapping through satellite remote sensing. Proc. 6th Asian Conf. Remote Sensing, Hyderabad, Nov. 21-26, pp. 77–83.

Lee JS, Jurkevich I, Dewaele P, Wambacq P and Oosterlinck A (1994) Speckle filtering of synthetic aperture radar images: a review. Remote Sensing Reviews 8 (4): 313–340.

Lillesand, T. M., and Kiefer, R. W., 1979. Remote Sensing and Image Interpretation (1st edit). John Willey and Sons, New York, USA.

Maktav, D., Erbek, F. S., and Jurgens, C., 2005. Remote sensing of urban areas. International Journal of Remote Sensing. 26 (4), pp. 655–659.

Neumann, M., Ferro Famil, L., 2008. Recent Advances in the Derivation of POL-inSAR Statistics: Study and Applications. 7th European Conference on Synthetic Aperture Radar, pp. 1–4, Friedrichshafen, Germany

Nyoungui, A. N., Tonye, E., and Akono, A., 2002. Evaluation of speckle filtering and texture analysis methods for land cover classification from SAR images. International Journal of Remote Sensing, 23 (9), pp. 1895–1925.

Paul Mather and Tso Brandt., 2009. Classification Methods for Remotely Sensed Data.Taylor & Francis, New York.

Qin, M., 2013. Application of RADARSAT-2 polarimetric data for land use and land cover classification and crop monitoring in southwestern Ontario. M.Sc. Thesis, University of Western Ontario London, Canada.

Quinlan, B., Huybrects, C., Schmidt, C., and Skiles, J. W., 2006. Detecting waste tire piles using high-resolution satellite imagery and an image processing model in two regions of California. ASPRS 2006 Annual Conference Reno, Nevada May 1-5, 2006.

Rebecca, M., (2003) Refinement of Automated Forest Area Estimation via Iterative Guided Spectral Class Rejection, M.Sc. Thesis, Virginia Polytechnic Institute and State University Blacksburg, Virginia

Wacker, A. G., and Landgrebe, D. A., 1972. Minimum distance classification in remote sensing. Report LARC Tech Report, Purdue University Lafayette, Indiana.

Wang, J. Z., Qu J. J., Zhang, W. M., and Zhang, K. C., 2016. Classification of full-polarization ALOS-PALSAR imagery using SVM in arid area of Dunhuang. Sciences in Cold and Arid Regions, 8 (3), pp. 263–267.

Yamada, H., K. Sato, Y. Yamaguchi, and W.-M. Boerner (2002), Interferometric phase and coherence of forest estimated by ESPRIT-based polarimetric SAR interferometry, IEEE International Geoscience and Remote Sensing Symposium. 2, pp. 829–831.

Yamaguchi, Y., Moriyama, T., Ishido, M., and Yamada, H., 2005. Four component scattering model for polarimetric SAR image decomposition. IEEE Transactions on Geoscience and Remote Sensing, 43 (8), pp. 1699–1706.

Yamada, H., Komaya, R., Yamaguchi, Y., and Sato, R., 2009. Scattering component decomposition for PolInSAR dataset and its applications. IEEE International Geoscience and Remote Sensing Symposium. 1, PP. 4–5.